Probing the electromagnetic dipole moment of the τ lepton in the $e^+e^- \to \gamma^*/Z \to \tau^+\tau^-$ reaction

Peng-Cheng Lu,* Zong-Guo Si,† and Han Zhang‡
School of Physics, Shandong University, Jinan, Shandong 250100, China

(Received 27 June 2025; accepted 3 October 2025; published 21 October 2025)

High-precision measurements of the lepton's electromagnetic dipole moments provide a powerful probe for testing the Standard Model. A nonzero value of the τ lepton's electric(weak) dipole moment (d_τ^γ, d_τ^Z) would serve as a smoking gun of the new physics. On the one hand, current and future high energy colliders offer an ideal environment for such measurements. On the other hand, it is essential to investigate the optimal measurement method for extracting not only d_τ^γ and d_τ^Z, but also the anomalous magnetic dipole moment (a_τ). In this work, we analyze the precision of observables, particularly optimal observables, for determining these physics quantities through the process $e^+e^- \to \gamma^*/Z \to \tau^+\tau^-$ with τ leptons undergoing (semi)leptonic and hadronic decays at the center-of-mass energies at the Z pole mass and significantly below m_Z. By considering the full kinematic information of the decay products, we find that the sensitivities to the weak dipole moments, $\mathrm{Im}[d_\tau^Z]$ and $\mathrm{Re}[d_\tau^Z]$, can reach 10^{-21} e cm at CEPC with $\sqrt{s} = m_Z$. This compares to sensitivities for the electric dipole moments, $\mathrm{Im}[d_\tau^\gamma]$ and $\mathrm{Re}[d_\tau^\gamma]$, of 10^{-20} e cm at Belle-II $\Upsilon(4S)$ resonance and 10^{-17} e cm at BEPCII $\psi(2S)$ resonance. For a_τ, we find that precisions of 10^{-5} for $\mathrm{Im}[a_\tau]$ and $\mathrm{Re}[a_\tau]$ can be attained at Belle-II $\sqrt{s} = 10.58$ GeV.

DOI: 10.1103/hvz6-b69m

I. INTRODUCTION

The search for electric dipole moments (EDM) and weak dipole moments (WDM) of fundamental fermions is an important aspect of experimental investigations hunting for physics beyond the Standard Model (SM) of particle physics, in particular for charge-parity (CP) violation beyond the Kobayashi-Maskawa mechanism (KM) [1]. In SM, EDMs, and WDMs of leptons induced by loop corrections are too small ($|d_\tau| \sim 10^{-38}$ e cm) [2,3] to be observed by current and near-future experiments. Any observation of a nonzero value for the EDM and/or WDM of an elementary particle would be a smoking gun evidence of non-SM sources of CP violation. Stringent upper limits on the EDM of the electron and muon have been obtained which are $|d_e| \leq 4.1 \times 10^{-30}$ e cm [4] and $|d_\mu| \leq 1.9 \times 10^{-19}$ e cm [5]. Sizable EDMs of heavy fermions, i.e., of the τ lepton can be generated in some models beyond the SM (BSM) [6], which might be detectable in the near future. However, due to short mean lifetime of the τ lepton, around 2.9×10^{-13} s [7], it decays too fast to be detected by using standard spin precession techniques, but searches using other methods can be carried out at the colliders. The most precise determination of the EDM of the τ lepton was obtained at Belle using $e^+e^- \to \tau^+\tau^-$ events with 833 fb^{-1} data sample [8], which read, for the real and imaginary component, respectively

$$\begin{aligned} \mathrm{Re}[d_\tau^\gamma] &= (-6.2 \pm 6.3) \times 10^{-18}\ e\,\mathrm{cm}, \\ \mathrm{Im}[d_\tau^\gamma] &= (-4.0 \pm 3.2) \times 10^{-18}\ e\,\mathrm{cm}. \end{aligned} \tag{1}$$

For the measurement on WDM of the τ lepton, the current best search results come from LEP, by measuring the transverse and normal τ lepton polarization [9]

$$\begin{aligned} \mathrm{Re}[d_\tau^Z] &= (-0.65 \pm 1.49) \times 10^{-18}\ e\,\mathrm{cm}, \\ \mathrm{Im}[d_\tau^Z] &= (0.4 \pm 3.8) \times 10^{-18}\ e\,\mathrm{cm}. \end{aligned} \tag{2}$$

The anomalous magnetic dipole moments (AMDM) of leptons, defined as $a_l = (g-2)/2$, are also used as probes of new physics (NP). In the SM, a_ℓ is generated by radiative corrections whose leading order (LO) contribution is given by the so-called Schwinger term $a_l^{(\mathrm{LO,SM})} = \alpha/(2\pi)$. a_e shows one of the best agreements between the SM prediction and the experimental result with

*Contact author: pclu@sdu.edu.cn
†Contact author: zgsi@sdu.edu.cn
‡Contact author: han.zhang@mail.sdu.edu.cn

Published by the American Physical Society under the terms of the Creative Commons Attribution 4.0 International license. Further distribution of this work must maintain attribution to the author(s) and the published article's title, journal citation, and DOI. Funded by SCOAP³.

precision up to 10 significant digits [10,11]. The Muon g-2 collaboration published the value of a_μ by combining the previous results given in [12–14], which showed a 5.1σ discrepancy between the theory prediction [15] and these experiments [16]. Based on lattice QCD calculation and a new τ-data-driven analysis, these discrepancies decrease to less than 2σ [17,18]. Very recently, this tension was removed in Ref. [19]. Since many BSM theories predict lepton's AMDM corrections scaling as $\delta a_l \propto \frac{m_l^2}{\Lambda^2}$ [20], the τ lepton exhibits enhanced sensitivity to the BSM effects compared to lighter leptons. Currently, the most stringent constraint for a_τ is obtained at the Large Hadron Collider (LHC) by the CMS collaboration using proton-proton collisions [21]. The resulting constraint on a_τ reads

$$-0.0042 < a_\tau < 0.0062, \quad 95\%\text{CL}. \tag{3}$$

On the other hand, the SM prediction is $a_\tau^{\text{SM}} = 117717.1 \pm 3.9 \times 10^{-8}$ [22].

The high-energy, high-luminosity colliders—notably Belle-II at SuperKEKB [23,24], Beijing Electron-Positron Collider II (BEPCII) [25,26], and the future Circular Electron-Positron Collider (CEPC) [27,28]—will enable precision measurements of the τ lepton's electromagnetic dipole moments through a huge amount of τ-pair production. The reaction $e^+e^- \to \tau^+\tau^-$ is particularly suitable for probing these quantities when colliders run at the center-of-mass (c.m.) energies of Z pole or significantly below m_Z. Assuming the scale of NP lies above the energy transfer of the process, the effective field theory allows the $\gamma\tau\tau$ and $Z\tau\tau$ vertex modifications, measured via this reaction, to be interpreted as the constrains on the d_τ and a_τ.

A possible way to improve the measurement precision of small physical parameters, i.e., d_τ and a_τ, involves constructing proper experimental observables with enhanced sensitivity. While straightforward observables utilize the kinematic variables of the detected final states, optimal observable minimize the statistical uncertainties in the measurement through maximum likelihood estimation [29,30]. Such observables have been extensively used in previous studies, including searches for the CP properties in Higgs boson interactions at LHC [31–33] and studies of anomalous charged triple gauge couplings [34,35]. In the context of probing the electric(week) dipole moment (E(W)DM) and AMDM of τ lepton, Ref. [36] investigated both real and imaginary components of τ EDM in τ-pair production via e^+e^- collisions at Belle-II; Ref. [37] explored the EDM and AMDM of τ lepton at same energy region while neglecting the imaginary components; Ref. [38] studied d_τ^γ at low-energy e^+e^- colliders using one-prong τ lepton decays channels; Ref. [39] probed optimal measurements of electromagnetic dipole moments of the τ lepton in PbPb collisions at LHC. Additionally, Refs. [40–42] utilized angle distributions to analyze the impact of the real component of τ EDM.

In this study, we investigate the E(W)DM and AMDM of the τ lepton through $e^+e^- \to \gamma^*/Z \to \tau^+\tau^-$ process, followed by the subsequent (semi)leptonic and hadronic decays of the τ leptons, and estimate the sensitivity for these dipole moments at both the Z pole energy and lower energies in e^+e^- collisions. This paper is structured as follows. In Sec. II we derive the production and decay spin density matrix for $e^+e^- \to \tau^+\tau^-$ incorporating the τ lepton's (semi)leptonic and hadronic decay channels. Recalling the form factor decomposition of the $\tau^+\tau^-V$ vertex, (V = γ, Z) and its relevant symmetry properties, we then turn to the observables in Sec. III, constructing simple and optimal observables to probe the electromagnetic dipole moment and analyzing the expectation values and covariances of these observables. Section IV presents our numerical results, including the estimates of the sensitivity for the measurement of real and imaginary components of E(W)DM and AMDM using observables defined in Sec. III. Comparisons are made across collider energy regimes. We summarize in Sec. V. The detailed numerical results are present in the Appendix.

II. THE REACTION

We consider $\tau^+\tau^-$ production in e^+e^- collisions via a virtual γ and Z boson, decaying into final states A and $\bar{B}$, respectively,

$$e^-(p_1) + e^+(p_2) \to \tau^-(k_1,\alpha) + \tau^+(k_2,\beta) \to A + \bar{B}. \tag{4}$$

The four-momenta and the corresponding three-momenta of electron and τ leptons are denoted in the e^+e^- c.m. frame by $p_{1,2} = (p^0_{1,2}, \mathbf{p}_{1,2})$, $k_{1,2} = (k^0_{1,2}, \mathbf{k}_{1,2})$. We consider unpolarized electrons and positrons and neglect their masses, the labels α, β denote the spin indices of the τ leptons. In this process, the general form factors for $\tau\tau\gamma$ and $\tau\tau Z$ vertex functions can be written in the form

$$\begin{aligned}\Gamma^\mu_{\tau\tau\gamma}(q^2) &= -ieQ_\tau\left(\gamma^\mu + \frac{\sigma_{\mu\nu}q^\nu}{2m}[iF_1(q^2) + F_2(q^2)\gamma_5]\right),\\ \Gamma^\mu_{\tau\tau Z}(q^2) &= \frac{g_Z}{2}\left(\gamma^\mu(V_\tau - \gamma_5 A_\tau)\right.\\ &\quad\left. + \frac{\sigma_{\mu\nu}q^\nu}{2m}[iG_1(q^2) + G_2(q^2)\gamma_5]\right),\end{aligned} \tag{5}$$

where m is the mass of the τ lepton and eQ_τ is the τ^- charge, g_Z is weak coupling constant, $\sigma_{\mu\nu} = i[\gamma_\mu, \gamma_\nu]/2$ and $q = k_1 + k_2$. The couplings associated with the form factors $F_1(q^2)$ and $G_1(q^2)$ are CP conserving, while those for $F_2(q^2)$ and $G_2(q^2)$ are CP violating. In the limit of $q^2 \to 0$, $F_1(q^2)$ corresponds to the electric anomalous magnetic dipole moment of $\tau^\pm$ (a_τ^γ), and $F_2(q^2)$ yields the electric dipole moment (d_τ^γ). The weak form factors $G_1(0)$ and $G_2(0)$ define the weak anomalous magnetic

dipole moment (a_τ^Z) and weak electric dipole moment (d_τ^Z) respectively. In our analysis, we shall consider the a_τ^V and d_τ^V (V = γ, Z) to be complex, with their imaginary parts being connected with the absorptive part of the vertex. At tree level in the SM, $a_\tau^V = 0$. Anomalous magnetic moment can have contributions both from NP and electroweak radiative corrections in the SM, thus $a_\tau^V = a_\tau^{V,\mathrm{SM}} + a_\tau^{V,\mathrm{NP}}$. As the electric dipole form factor in the SM is highly suppressed, one can assume that this form factor comes exclusively from NP contributions, that is $d_\tau^V = d_\tau^{V,\mathrm{NP}}$.

For on-shell τ pair production and decay in the reaction (4), the total cross section with Eq. (5) for $\tau\tau V$ couplings is given by the product of the production density matrix $\chi_{\alpha\alpha'\beta\beta'}$ for $e^+e^- \to \tau^+\tau^-$ and the density matrices $\mathcal{D}^a_{\beta'\beta}$ and $\mathcal{D}^{\bar{b}}_{\alpha'\alpha}$ that describe the decays of polarized $\tau^- \to A \to a(q_-) + X$ and $\tau^+ \to \bar{B} \to \bar{b}(q_+) + X'$, respectively. The narrow width approximation of the intermediate τ leptons is used. Thus the differential cross section can be written as

$$d\sigma_{a\bar{b}} = \frac{1}{2s}\chi_{\alpha\alpha'\beta\beta'}\mathcal{D}^a_{\beta'\beta}\mathcal{D}^{\bar{b}}_{\alpha'\alpha}d\phi, \tag{6}$$

where $s = (p_1 + p_2)^2$ and $d\phi$ is the usual phase space measure. We expand the production density matrix of the τ lepton to first order in the dipole and anomalous magnetic moment form factors, neglecting the spin indices

$$\begin{aligned}\chi_{\mathrm{prod}} = \chi_0 &+ \mathrm{Re}[d_\tau^V]\chi_{\mathrm{Re}d} + \mathrm{Im}[d_\tau^V]\chi_{\mathrm{Im}\,d} \\ &+ \mathrm{Re}[a_\tau^{V,NP}]\chi_{\mathrm{Re}a} + \mathrm{Im}[a_\tau^{V,NP}]\chi_{\mathrm{Im}\,a} \\ &+ \mathcal{O}((a_\tau^V)^2, (d_\tau^V)^2),\end{aligned} \tag{7}$$

where χ_0 is the SM term where $d_\tau^V = 0$ and $a_\tau^{V,NP} = 0$. χ_{Red} and χ_{Imd} are the interference terms between SM and NP-induced E(W)DM for the real and imaginary components of d_τ, while χ_{Rea} and χ_{Ima} are the interference terms between SM and NP-induced AMDM for the real and imaginary components of a_τ. We neglect the higher order term of d_τ^V and a_τ^V since they are small. The tree level $\chi_{0,\mathrm{tree}}$ is CP even and naive-CPT even. Once the electroweak correction is considered, this term may become naive-CPT odd but CP even. T even or odd refers to the behavior under naive time reversal transformation, which reverses particle momenta and spins but does not interchange initial and final states.

For the decay channels, we consider τ pair events in two cases:

(i) One-prong decays: Only one charged particle from each of A and $\bar{B}$ is measured. Including $\tau^- \to \ell^-(q_-)\nu\nu$ ($\ell = e, \mu$), $\pi^-(q_-)\nu$, $\rho^-(q_-)\nu$, along with the charge-conjugate τ^+ decay.

(ii) Multiprong decays: More than one particle from each of A and $\bar{B}$ are measured. Including $\tau^- \to \pi^-(q_1)\pi^0(q_2)\nu$, $\pi^-(q_1)\pi^-(q_2)\pi^+(q_3)\nu$, along with the charge-conjugate τ^+ decay.

After integrating the energy of the charged particle $a^\pm$ that acts as $\tau^\pm$ spin analyzer, the decay density matrix in the τ rest frame for one charged prong case can be written as

$$\frac{d^3q_\pm}{(2\pi)^3 2q_\pm^0}\mathcal{D}^{a^\pm}_{\beta'\beta}[\tau^\pm \to a^\pm(q_\pm) + X] = \frac{d\Omega_{a^\pm}}{4\pi}[1 + \alpha_a \hat{q}_\pm \cdot \sigma], \tag{8}$$

where $d\Omega_{a^\pm}$ is the solid angle of $a^\pm$. α_a is the spin-analyzing power of τ lepton. In the SM, it is well known that the π and ρ have high spin analyzing power, with $\alpha_\pi = 1$ and $\alpha_\rho = 0.45$. The decay density matrices for polarized $\tau^\pm$ in several major decay channels have been calculated in [36].

III. OBSERVABLES

In this section, we discuss the simple observables and the so-called optimal observables, along with their sensitivities for determining the values of d_τ^V and $a_\tau^{V,NP}$. We decompose the differential cross section of the reaction(4) according to g_j, neglecting terms quadratic in g_j

$$\begin{aligned}d\sigma_{a\bar{b}} = (&S_0 + S_{1,\mathrm{Re}d_\tau}\mathrm{Re}[d_\tau^V] + S_{1,\mathrm{Im}\,d_\tau}\mathrm{Im}[d_\tau^V] \\ &+ S_{1,\mathrm{Re}a_\tau}\mathrm{Re}[a_\tau^{V,NP}] + S_{1,\mathrm{Im}\,a_\tau}\mathrm{Im}[a_\tau^{V,NP}])d\phi,\end{aligned} \tag{9}$$

here g_j ($j = 1, 2, 3$, and 4) represents the quantities $\mathrm{Re}[d_\tau^V]$, $\mathrm{Im}[d_\tau^V]$, $\mathrm{Re}[a_\tau^{V,NP}]$, and $\mathrm{Im}[a_\tau^{V,NP}]$ to be determined. Determination of these quantities requires choosing four observables $\mathcal{O}_i$ and measure their expectation values in the same experimental run

$$E[\mathcal{O}_i] = E_0[\mathcal{O}_i] + \sum_j c_{ij}g_j, \tag{10}$$

$E_0[\mathcal{O}_i]$ denotes the expectation value without contributions from g_j and c_{ij} is the coefficient matrix that specifies the relationship between $E[\mathcal{O}_i]$ and the g_j. The goal is to measure g_j as accurately as possible. Consider a set of unbiased estimators, denoted as γ_i, defined as $\gamma_i = \sum_j c_{ij}^{-1}(E[\mathcal{O}_i] - E_0[\mathcal{O}_i])$. The expectation values for these estimators are $E[\gamma_i] = g_i$. Expanding in g_j gives

$$\begin{aligned}E[\mathcal{O}_i] = &\frac{\int d\phi S_0 \mathcal{O}_i}{\int d\phi S_0} \\ &+ \sum_j \left(\frac{\int d\phi S_{1,j}\mathcal{O}_i}{\int d\phi S_0} - \frac{\int d\phi S_0 \mathcal{O}_i \int d\phi S_{1,j}}{(\int d\phi S_0)^2}\right) g_j.\end{aligned} \tag{11}$$

To further assess the sensitivity of observables to those small couplings, one must compare with the errors in the measurement of expectation of observables. If N events are recorded, these error will be given by $\sqrt{V(\mathcal{O})_{ij}/N}$, with

$$V(\mathcal{O})_{ij} = \frac{d\phi S_0 \mathcal{O}_i \mathcal{O}_j}{\int d\phi S_0} - \frac{\int d\phi S_0 \mathcal{O}_i \int d\phi S_0 \mathcal{O}_j}{(\int d\phi S_0)^2} \quad (12)$$

being the covariance matrix of the quantities $\mathcal{O}$ for $g_j = 0$. This matrix is symmetric and positive semi-definite and will be a diagonal matrix in the case of all $\mathcal{O}$ being uncorrelated observables. Thus, the one-sigma standard deviation or the so-called background-to-signal ratio δg_i, with which the presence of nonzero g_i can be ascertained reads

$$\delta g_i = \frac{1}{|c_{ij}|} \sqrt{\frac{V(\mathcal{O})_{ij}}{N}}. \quad (13)$$

We now discuss the four optimal observables which reads

$$\mathcal{O}_i = \frac{S_{1,i}}{S_0}, (i = \mathrm{Re}d_\tau, \mathrm{Im}\, d_\tau, \mathrm{Re}a_\tau, \mathrm{Im}\, a_\tau) \quad (14)$$

that can optimize the signal-to-background ratio in the measurements [29,30]. $S_{1,i}$ and S_0 are the differential cross section defined by Eq. (9). Clearly, optimal observables inherit whatever discrete asymmetries $S_{1,i}$ has with respect to S_0. In this work, it is suitable to define observables especially CP odd observables in terms of process (4) and its charge conjugated decays. The expectation value of the observables of interest are defined as the following average

$$E^{ab}[\mathcal{O}] = \frac{1}{2}\left(\frac{\int d\sigma_{a\bar{b}} \mathcal{O}}{\int d\sigma_{a\bar{b}}} + \frac{\int d\sigma_{b\bar{a}} \mathcal{O}}{\int d\sigma_{b\bar{a}}}\right), \quad (15)$$

where $d\sigma_{b\bar{a}}$ is the differential cross section for the charge-conjugate process of reaction (4). These optimal observables share the same transformation properties under CP and T as the couplings. Specifically, observables sensitive to the $\gamma\tau\tau$ couplings will also be sensitive to the corresponding $Z\tau\tau$ couplings. For example, the expectation value of CP odd observables can only project CP odd term of the differential cross section in Eq. (9). Consequently, for CP even SM contribution, any nonzero expectation value for a CP odd observable serves as a clear signal of CP violation in the reaction. The reverse is also true: CP even term of differential cross section do not contribute to the expectation value of CP odd observable. The discussion here assumes the phase space cuts in experimental measurements are CP blind.

In addition to optimal observables, we also study simple observables constructed solely from the momenta of the decay products of $\tau^+\tau^-$. For the case of the imaginary and real E(W)DM couplings, we choose simple observables of the form

$$\begin{aligned} T^{ij} &= (\mathbf{q}_+ - \mathbf{q}_-)^i (\mathbf{q}_+ \times \mathbf{q}_-)^j + (i \leftrightarrow j), \quad \text{odd under CP; odd under T,} \\ \hat{O}^{ij} &= (\hat{\mathbf{q}}_+ + \hat{\mathbf{q}}_-)^i (\hat{\mathbf{q}}_+ - \hat{\mathbf{q}}_-)^j + (i \leftrightarrow j), \quad \text{odd under CP; even under T,} \end{aligned} \quad (16)$$

which have the same symmetry as $S_{1,\mathrm{Re}d_\tau}$ and $S_{1,\mathrm{Im}\, d_\tau}$. Here, $\mathbf{q}_\pm$ are the three-momenta of the final states defined in the e^+e^- frame, $\hat{\mathbf{q}}_\pm = \mathbf{q}_\pm/|\mathbf{q}_\pm|$ and i, j are the Cartesian vector indices. For the case of real and imaginary AMDM couplings, we consider simple observables of the form

$$T_a^{ij} = (\mathbf{q}_+ + \mathbf{q}_-)^i (\mathbf{q}_+ \times \mathbf{q}_-)^j + (i \leftrightarrow j), \quad \text{even under } CP\text{; odd under T,} \quad (17)$$

and

$$\hat{O}_a^{ij} = \hat{\mathbf{q}}_+^i \cdot \hat{\mathbf{q}}_-^j + (i \leftrightarrow j), \quad \text{even under CP; even under T,} \quad (18)$$

which have the same symmetry as $S_{1,\mathrm{Im}\, a_\tau}$ and $S_{1,\mathrm{Re}a_\tau}$. Besides above tensor simple observables, vector observables are essential to project the contributions arising from the interference of vector and axial couplings [43]. Based on the kinematic structures of these interference terms, the vector observables take the form

$$\begin{aligned} \hat{A}_1 &= \hat{\mathbf{p}} \cdot \frac{\hat{\mathbf{q}}_+ \times \hat{\mathbf{q}}_-}{|\hat{\mathbf{q}}_+ \times \hat{\mathbf{q}}_-|}, \quad \text{odd under CP; odd under T,} \\ \hat{A}_2 &= \hat{\mathbf{p}} \cdot (\hat{\mathbf{q}}_+ - \hat{\mathbf{q}}_-), \quad \text{odd under CP; even under T.} \end{aligned} \quad (19)$$

where $\hat{\mathbf{p}}$ denotes the unit vector of the electron momentum in e^+e^- c.m. frame.

IV. NUMERICAL RESULTS

We consider $\tau^+\tau^-$ production and their decay in e^+e^- collisions and compute the expectation values of the simple and optimal observables defined in the previous section. We also discuss the one-sigma sensitivities to the E(W)DM and AMDM form factors $\mathrm{Re}[d_\tau^V]$, $\mathrm{Im}[d_\tau^V]$, $\mathrm{Re}[a_\tau^{V,NP}]$, and $\mathrm{Im}[a_\tau^{V,NP}]$. These expectation values are computed using the production density matrix in Eq. (7) and τ leptons decay density matrix. No phase space cuts are applied.

In the case $a = b$, as discussed above, for the CP odd observables, only the term corresponding to the CP odd differential cross section contributes to their expectation value. This is a direct consequence of the CP symmetry properties, which imply

$$E_0^{a\bar{a}}[\mathcal{O}_{\mathrm{Re}d_\tau}] = 0, \quad E_0^{a\bar{a}}[\mathcal{O}_{\mathrm{Im}\,d_\tau}] = 0, \tag{20}$$

$$E_0^{a\bar{a}}[T^{ij}] = 0, \quad E_0^{a\bar{a}}[\hat{O}^{ij}] = 0. \tag{21}$$

The cross-term drops out by further applying T symmetry properties, which imply

$$E_0^{a\bar{a}}[\mathcal{O}_{\mathrm{Re}d_\tau}\mathcal{O}_{\mathrm{Im}\,d_\tau}] = 0, \quad E_0^{a\bar{a}}[T^{ij}\hat{O}^{ij}] = 0. \tag{22}$$

Thus, the covariance matrix and coefficient matrix are both diagonal. For cases where $a \neq b$, applying the T transformation results in the following SM expectation values:

$$E_0^{a\bar{b}}[\mathcal{O}_{\mathrm{Re}d_\tau}] = 0, \quad E_0^{a\bar{b}}[T^{ij}] = 0,$$
$$E_0^{a\bar{b}}[\mathcal{O}_{\mathrm{Re}d_\tau}\mathcal{O}_{\mathrm{Im}\,d_\tau}] = 0, \quad E_0^{a\bar{b}}[T^{ij}\hat{O}^{ij}] = 0, \tag{23}$$

while $E_0^{a\bar{b}}[\hat{O}^{ij}] \neq 0$, $E_0^{a\bar{b}}[\mathcal{O}_{\mathrm{Im}\,d_\tau}] \neq 0$. This behavior arises because the final states are no longer CP symmetric in such cases. Consequently, the average observables defined in Eq. (15) are used. With the CP property of $\hat{O}^{ij}$ and $\mathcal{O}_{\mathrm{Im}\,d_\tau}$, we obtain

$$E_0^{ab}[\hat{O}^{ij}] = 0, \quad E_0^{ab}[\mathcal{O}_{\mathrm{Im}\,d_\tau}] = 0. \tag{24}$$

Any nonzero value of $E^{ab}[\mathcal{O}]$ may be regarded as a potential signal of the NP.

For the process where τ decays into three π, the $E_0^{ab}[\mathcal{O}_{\mathrm{Re}d_\tau}\mathcal{O}_{\mathrm{Im}\,d_\tau}] \neq 0$ is induced by absorptive parts originating from the finite widths of the intermediate resonances. However, this term is significantly smaller compared to our numerical uncertainties and can thus be safely neglected. Again $E_0^{ab}[\mathcal{O}_{\mathrm{Re}d_\tau}] = 0$ and $E_0^{ab}[\mathcal{O}_{\mathrm{Im}\,d_\tau}] = 0$ hold in this 3π process.

Now, we consider the expectation values of CP even observables. Since the SM expectation value of $\mathcal{O}_{\mathrm{Im}\,a_\tau}$ and $\mathcal{O}_{\mathrm{Re}a_\tau}$ are not equal to zero, we utilize the general relationship between expectation values of observables and the values of $a_\tau^{V,NP}$ as defined in Eq. (11).

Based on the above discussion, the expectation values of the CP-odd simple observables in Eq. (16) for E(W)DM are of the form

$$\begin{pmatrix} E^{ab}[T^{ij}] \\ E^{ab}[\hat{O}^{ij}] \end{pmatrix} = \begin{pmatrix} c_{ab} & 0 \\ 0 & \bar{c}_{ab} \end{pmatrix} \begin{pmatrix} \mathrm{Re}[\hat{d}_\tau^V]s^{ij} \\ \mathrm{Im}[\hat{d}_\tau^V]s^{ij} \end{pmatrix}, \tag{25}$$

with dimensionless E(W)DM form factors defined by

$$\mathrm{Re}[\hat{d}_\tau^V] = \frac{\sqrt{s}}{e}\mathrm{Re}[d_\tau^V], \quad \mathrm{Im}[\hat{d}_\tau^V] = \frac{\sqrt{s}}{e}\mathrm{Im}[d_\tau^V], \tag{26}$$

while those of the CP-even simple observables in Eqs. (17) and (18), which probe AMDM, are of the form

$$\begin{pmatrix} E^{ab}[T_a^{ij}] \\ E^{ab}[\hat{O}_a^{ij}] \end{pmatrix} = \begin{pmatrix} k_{a\bar{b}}^{11} & k_{a\bar{b}}^{12} \\ \bar{k}_{a\bar{b}}^{21} & \bar{k}_{a\bar{b}}^{22} \end{pmatrix} \begin{pmatrix} \mathrm{Im}[a_\tau^{V,NP}]s^{ij} \\ \mathrm{Re}[a_\tau^{V,NP}]s^{ij} \end{pmatrix} + \begin{pmatrix} E_0^{ab}[T_a^{ij}] \\ E_0^{ab}[\hat{O}_a^{ij}] \end{pmatrix} \tag{27}$$

where s_{ij} is the tensor polarization of the intermediate γ/Z state, which can be written as $\mathrm{diag}(-\frac{1}{6}, -\frac{1}{6}, \frac{1}{3})$ if the beam direction is identified with the z-axis. When the coefficient matrix is not diagonal in Eq. (27), using the whitening transformation to decorrelate the observables, one can find a linearly approximated optimal basis out of the original chosen ones. The resulting ideal one standard deviation (1 s.d.) sensitivity of the E(W)DM couplings are given by

$$\delta\mathrm{Red}_\tau = \frac{e}{\sqrt{s}}\frac{1}{\sqrt{N_{ab}}}\frac{3[E_0^{ab}[T_{33}^2]]^{1/2}}{|c_{ab}|},$$
$$\delta\mathrm{Imd}_\tau = \frac{e}{\sqrt{s}}\frac{1}{\sqrt{N_{ab}}}\frac{3[E_0^{ab}[\hat{O}_{33}^2]]^{1/2}}{|\bar{c}_{ab}|}, \tag{28}$$

where $N_{ab} = 2N_{\tau\tau}\mathrm{Br}(\tau \to a)\mathrm{Br}(\tau \to b)$ with $N_{\tau\tau}$ being the number of τ pair events. After the diagonalization operation of the covariance matrix, the 1 s.d. sensitivity of the AMDM couplings can be written as

$$\delta\mathrm{Rea}_\tau = \frac{1}{\sqrt{N_{ab}}}\frac{3[V'_{ab}(\hat{O}_a^{33})]^{1/2}}{|\kappa_{ab}|},$$
$$\delta\mathrm{Ima}_\tau = \frac{1}{\sqrt{N_{ab}}}\frac{3[V'_{ab}(T_a^{33})]^{1/2}}{|\bar{\kappa}_{ab}|}, \tag{29}$$

where κ_{ab}, $\bar{\kappa}_{ab}$ are components of the new diagonal coefficient matrix and $V'_{ab}(\hat{O}_a^{33})$, $V'_{ab}(T_a^{33})$ are components of the new diagonal covariance matrix.

The expectation values of the optimal observables defined in Eq. (14) are of the form

$$\begin{pmatrix} E^{ab}[\mathcal{O}_{\mathrm{Re}d_\tau}] \\ E^{ab}[\mathcal{O}_{\mathrm{Im}\,d_\tau}] \end{pmatrix} = \begin{pmatrix} \omega_{ab} & 0 \\ 0 & \bar{\omega}_{ab} \end{pmatrix} \begin{pmatrix} \mathrm{Re}[\hat{d}_\tau^V] \\ \mathrm{Im}[\hat{d}_\tau^V] \end{pmatrix}, \tag{30}$$

and

$$\begin{pmatrix} E^{ab}[\mathcal{O}_{\mathrm{Re}a_\tau}] \\ E^{ab}[\mathcal{O}_{\mathrm{Im}\,a_\tau}] \end{pmatrix} = \begin{pmatrix} \xi^{11}_{a\bar{b}} & \xi^{12}_{a\bar{b}} \\ \xi^{21}_{a\bar{b}} & \xi^{22}_{a\bar{b}} \end{pmatrix} \begin{pmatrix} \mathrm{Im}[a_\tau^{V,NP}] \\ \mathrm{Re}[a_\tau^{V,NP}] \end{pmatrix} + \begin{pmatrix} E_0^{ab}[\mathcal{O}_{\mathrm{Re}a_\tau}] \\ E_0^{ab}[\mathcal{O}_{\mathrm{Im}\,a_\tau}] \end{pmatrix}. \tag{31}$$

The definition of the variables in the above expressions are similar to simple observables.

In the continuum above the Z-pole energy, the interference between γ and Z boson exchange mechanisms should be taken into account. As the real and imaginary components of electric and weak dipole form factors are to be determined at a fixed c.m. energy, we further decompose the differential cross section defined in Eq. (9) into the form

$$d\sigma_{a\bar{b}} = \sum_{V=\gamma,Z} (S_0^V + S^V_{1,\mathrm{Re}d_\tau}\mathrm{Re}[d_\tau^V] + S^V_{1,\mathrm{Im}\,d_\tau}\,\mathrm{Im}[d_\tau^V] + S^V_{1,\mathrm{Re}a_\tau}\mathrm{Re}[a_\tau^{V,NP}] + S^V_{1,\mathrm{Im}\,a_\tau}\,\mathrm{Im}[a_\tau^{V,NP}])d\phi, \tag{32}$$

where $V = \gamma$, Z. In this regime, the real and imaginary components of d_τ^γ and d_τ^Z cannot be determined independently. However, by a simultaneous measurement of T^{ij} and $\hat{A}_1$, the real components $\mathrm{Re}[d_\tau^\gamma]$ and $\mathrm{Re}[d_\tau^Z]$ can be disentangled. The expectation values of T^{ij} and $\hat{A}_1$ in the same experimental run are given by

$$\begin{pmatrix} E^{ab}[T^{ij}] \\ E^{ab}[\hat{A}_1] \end{pmatrix} = \begin{pmatrix} c_\gamma & c_Z \\ r_\gamma & r_Z \end{pmatrix} \begin{pmatrix} \mathrm{Re}[\hat{d}_\tau^\gamma]s^{ij} \\ \mathrm{Re}[\hat{d}_\tau^Z]s^{ij} \end{pmatrix}. \tag{33}$$

The 1 s.d. statistical sensitivities read

$$\delta\mathrm{Re}d_\tau^\gamma = \frac{e}{\sqrt{s}}\frac{1}{\sqrt{N_{ab}}}\frac{[E_0^{ab}[(3r_Z T_{33} - c_Z\hat{A}_1)^2]]^{1/2}}{|c_\gamma r_Z - c_Z r_\gamma|},$$
$$\delta\mathrm{Re}d_\tau^Z = \frac{e}{\sqrt{s}}\frac{1}{\sqrt{N_{ab}}}\frac{[E_0^{ab}[(3r_\gamma T_{33} - c_\gamma\hat{A}_1)^2]]^{1/2}}{|c_Z r_\gamma - c_\gamma r_Z|}, \tag{34}$$

and analogously for the imaginary components of the dipole form factors. The quantities c_V and γ_V are the components of the coefficient matrix, while the corresponding components of the coefficient matrix for $\hat{O}^{ij}$ and $\hat{A}_2$ are denoted as c'_V and γ'_V. The expectation values of optimal observables defined as $\mathcal{O}_i^V = S^V_{1,i}/S_0$, $(i = \mathrm{Re}d_\tau)$ are of the form

$$\begin{pmatrix} E^{ab}[\mathcal{O}^\gamma_{\mathrm{Re}d_\tau}] \\ E^{ab}[\mathcal{O}^Z_{\mathrm{Re}d_\tau}] \end{pmatrix} = \begin{pmatrix} w_\gamma & w_Z \\ t_\gamma & t_Z \end{pmatrix} \begin{pmatrix} \mathrm{Re}[\hat{d}_\tau^\gamma] \\ \mathrm{Re}[\hat{d}_\tau^Z] \end{pmatrix}, \tag{35}$$

and the 1 s.d. statistical sensitivities are given by

$$\delta\mathrm{Re}d_\tau^\gamma = \frac{e}{\sqrt{s}}\frac{1}{\sqrt{N_{ab}}}\frac{[E_0^{ab}[(t_Z\mathcal{O}^\gamma_{\mathrm{Re}d_\tau} - w_Z\mathcal{O}^Z_{\mathrm{Re}d_\tau})^2]]^{1/2}}{|w_\gamma t_Z - w_Z t_\gamma|},$$
$$\delta\mathrm{Re}d_\tau^Z = \frac{e}{\sqrt{s}}\frac{1}{\sqrt{N_{ab}}}\frac{[E_0^{ab}[(t_\gamma\mathcal{O}^\gamma_{\mathrm{Re}d_\tau} - w_\gamma\mathcal{O}^Z_{\mathrm{Re}d_\tau})^2]]^{1/2}}{|w_Z t_\gamma - w_\gamma t_Z|}, \tag{36}$$

The expectation values and corresponding 1 s.d. statistical sensitivities of $\mathcal{O}_i^V = S^V_{1,i}/S_0$, $(i = \mathrm{Im}\,d_\tau)$ are analogous to those in Eqs. (35) and (36), except that the coefficients are expressed in terms of w'_V and t'_V. Of course, Eqs. (33)–(36) simplify significantly at the Z resonance and for energies far below, where the weak and the electric dipole form factors can be determined independently from Eqs. (25) and (28).

For the numerical results to be presented below, the following input parameters are adopted

$$m = 1.777\ \mathrm{GeV}, \quad m_Z = 91.188\ \mathrm{GeV}, \quad m_W = 80.369\ \mathrm{GeV}, \quad m_\pi = 0.140\ \mathrm{GeV},$$
$$m_\rho = 0.775\ \mathrm{GeV}, \quad \Gamma_Z = 2.496\ \mathrm{GeV}, \quad G_\mu = 1.166\,379 \times 10^{-5}\ \mathrm{GeV}^{-2}. \tag{37}$$

The decay channels that we used in this study, along with their branching ratios and spin analyzing powers are shown in Table I.

TABLE I. Decay channels of τ^- with the corresponding branching ratios and spin analyzing power.

Decay channel	Spin analyzing power(α_a)	Branching ratio
$e^-/\mu^-(q_-)\nu\nu$	−0.33	17.4%
$\rho^-(q_-)\nu$	0.45	25.5%
$\pi^-(q_-)\nu$	1.00	10.8%
$\pi^-(q_1)\pi^0(q_2)\nu$	…	25.5%
$\pi^-(q_1)\pi^-(q_2)\pi^+(q_3)\nu$	…	9.31%

A. E(W)DM results

The EDM of the τ lepton can be effectively extracted from $e^+e^- \to \tau^+\tau^-$ at energies significantly lower than the Z boson mass, particularly near the $\tau^+\tau^-$ threshold. We consider τ pair production and decay at BEPCII that has been operating since 2009 whose c.m. energies ranging from $\sqrt{s} = 2.0$–4.94 GeV with an integrated luminosity of 35 fb^{-1} [26]. The largest dataset of the $\tau^+\tau^-$ events are from the $\psi(2S)$ resonance. In 2020, BEPCII plans to make two upgrades. One is increasing the maximum c.m. energy to 5.6 GeV. The other one is increasing the peak luminosity by a factor of 3 for c.m. energies from 4.0 to 5.6 GeV.

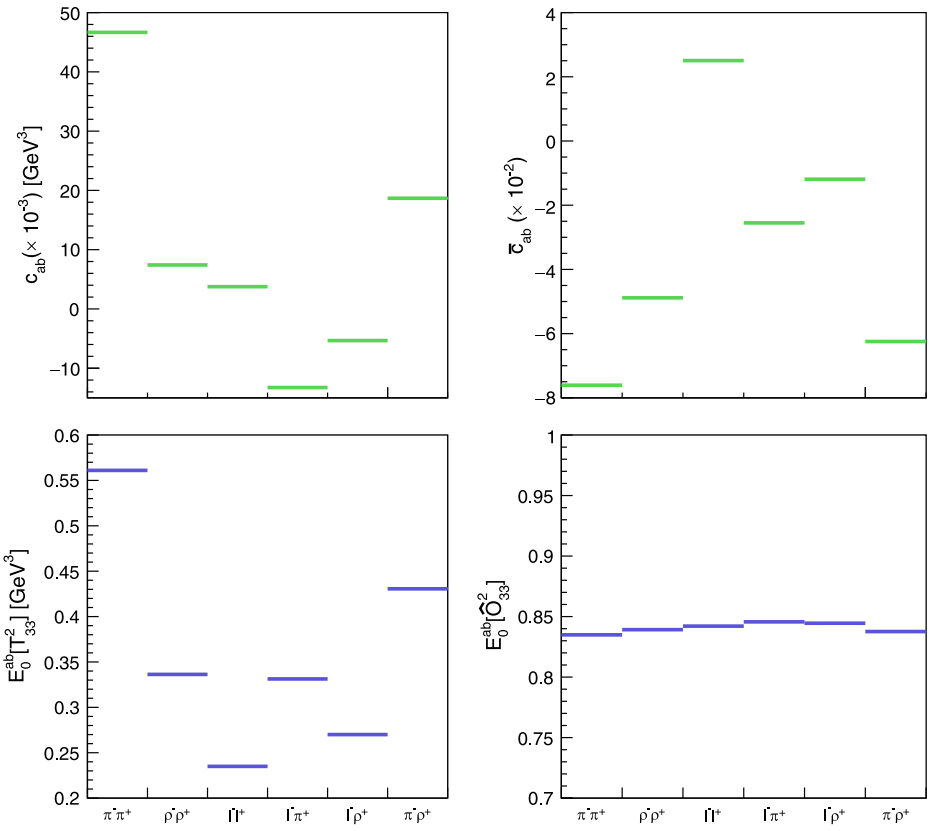


FIG. 1. Simple observables T^{ij} (left) and $\hat{O}^{ij}$ (right) at $\sqrt{s} = 3.686$ GeV. The upper panel shows our results for c_{ab} and $\bar{c}_{ab}$ defined in Eq. (25) while the lower panel exhibits the variances of the observables defined in Eq. (12). The x-axis represents the various decay modes. For the modes where leptons are involved the cross section is the sum of the respective cross sections for $\ell = e$ and μ.

Besides, we also consider c.m. energy from τ-pair threshold up to 15 GeV. In this energy regime, the Belle-II experiment will accumulate about 4.5×10^{10} τ pair at $\Upsilon(4S)$ resonance at $\sqrt{s} = 10.58$ GeV.

WDM of τ lepton can be best probed experimentally from the τ pair production at the Z resonance. The huge amount of produced $\tau^+\tau^-$ pairs at the Z resonance expected at CEPC, together with the improved τ- reconstruction efficiency will allow, among other investigations, the search for d_τ^Z with a precision expected to be significantly higher than existing bounds.

In summary, we consider the following four scenarios in this paper:

(i) Scenario I: $\sqrt{s} = 3.686$ GeV, the number of $\tau^+\tau^-$: $N_{\psi(2S)\to\tau^+\tau^-} = 3.5 \times 10^6$,
(ii) Scenario II: $\sqrt{s} = 5.6$ GeV, Integrated luminosity: $L = 20$ fb^{-1},
(iii) Scenario III: $\sqrt{s} = 10.58$ GeV, the number of $\tau^+\tau^-$: $N_{\Upsilon(4S)\to\tau^+\tau^-} = 4.5 \times 10^{10}$,
(iv) Scenario IV: $\sqrt{s} = m_Z$, the number of $\tau^+\tau^-$: $N_{Z\to\tau^+\tau^-} = 1.2 \times 10^{11}$.

Since we consider the normalized expectation values of observables, the resonance effects where the propagator receives an enhancement at the resonances $\psi(2S)$, $\Upsilon(4S)$ and the Z boson resonance, enters only through the number of τ lepton events, which serves as an input parameter. Figure 1 shows the results for the expectation values of the simple observables T^{ij} at the left panel and $\hat{O}^{ij}$ at the right panel in the scenario I assuming 3.5×10^6 produced τ pairs at $\sqrt{s} = 3.686$ GeV. The upper panel is the results of the coefficient matrix defined in Eq. (25), the values of which are expected to be large; while the lower panel is the variances of the observables in Eq. (12) and we expect their values to be small. The x-axis represents various decay modes of $\tau^+\tau^-$. The upper and lower panel can be seen as signal and background strength. As seen from the values in the upper panel, the $\pi^+\pi^-$ channel has the highest sensitivities to both $\mathrm{Re}[d_\tau^\gamma]$ and $\mathrm{Im}[d_\tau^\gamma]$. This is due to the high spin analyzing power of the π. Furthermore, channels with pions in the final state are more sensitive to $\mathrm{Re}[d_\tau^\gamma]$ than leptonic channels, while the $\hat{O}^{33}$ in $\rho^+\rho^-$ channel is more relevant to $\mathrm{Im}[d_\tau^\gamma]$ than leptonic and semileptonic decay channel of $\tau^+\tau^-$. From the lower panel, the measurement errors for $\mathrm{Re}[d_\tau^\gamma]$ in $\pi^+\pi^-$ and $\pi^-\rho^+$ are also large. The errors differences for measuring $\mathrm{Im}[d_\tau^\gamma]$ across various decay channels are relatively small.

Figure 2 presents the results for the expectation values of the optimal observables $\mathcal{O}_{\mathrm{Re}d_\tau}$ and $\mathcal{O}_{\mathrm{Im}\,d_\tau}$. The upper panel

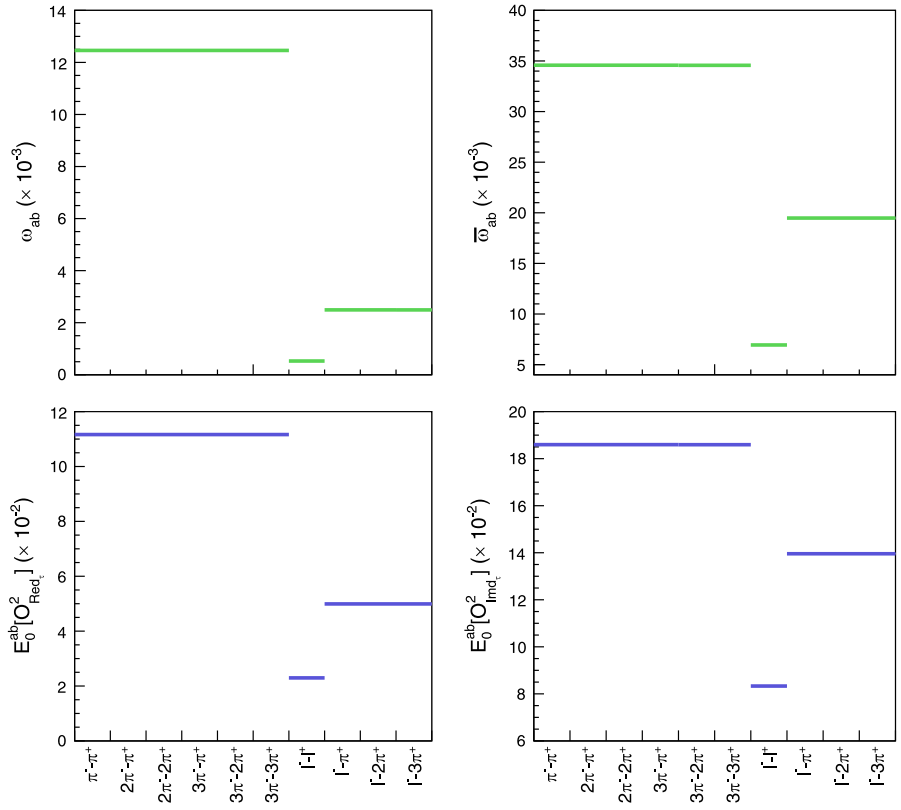


FIG. 2. Optimal observables $\mathcal{O}_{\mathrm{Re}d_\tau}$ (left) and $\mathcal{O}_{\mathrm{Im}\,d_\tau}$ (right) at $\sqrt{s} = 3.686$ GeV. The upper and lower panels show quantities analogous to Fig. 1.

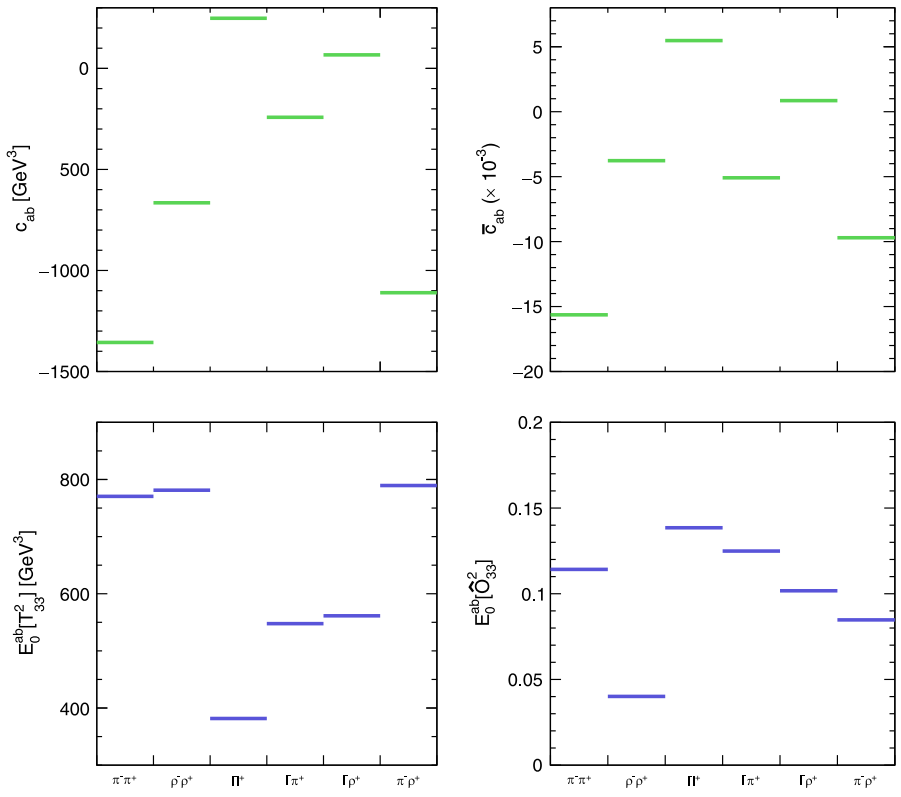


FIG. 3. Same as the Fig. 1, but at c.m. energy $\sqrt{s} = m_Z$.

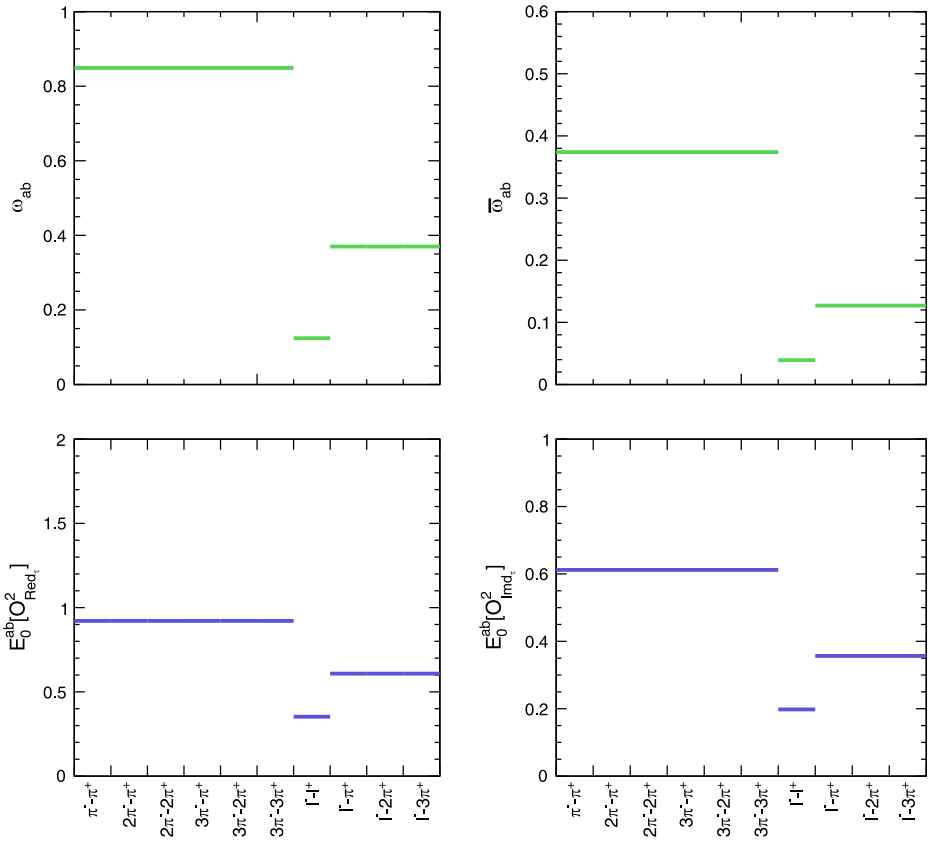


FIG. 4. Same as the Fig. 2, but at c.m. energy $\sqrt{s} = m_Z$.

shows that the sensitivity of these two observables in double-leptonic decay of τ pair are much lower than other decay modes. As shown in the lower panels, these optimal observables exhibit smaller statistical uncertainties than the simple observables in Fig. 1. Analogous behaviors are also observed for the scenario II and III. For the WDM of the τ lepton (scenario IV), Fig. 3 displays the results for simple observables. The $\rho^+\rho^-$ channel shows sensitivity to $\mathcal{O}_{\mathrm{Red}_\tau}$, complementing the previously noted $\pi^+\pi^-$ and $\pi^-\rho^+$ channels. The absolute values of coefficient c_{ab} are markedly larger than those in γ coupling. The statistical uncertainties of the optimal observables in Fig. 4 are smaller at $\sqrt{s} = m_Z$ than at lower energies.

Combining the statistical errors of the expectation values of the observables with the signal strength, we compute the 1 s.d. sensitivities shown in Table II for various scenarios. The results demonstrates significant precision improvements when using the optimal observables compared to the simple observables. At BEPCII's benchmark energies, $\sqrt{s} = 3.686$ GeV and $\sqrt{s} = 5.6$ GeV, the EDM sensitivity reaches 4.87×10^{-17} e cm and 2.93×10^{-18} e cm for the real component and 2.40×10^{-17} e cm and 1.42×10^{-18} e cm

TABLE II. 1 s.d. sensitivity on $\mathrm{Re}[d_\tau^V]$ and $\mathrm{Im}[d_\tau^V]$ in the combined decay channels.

	$\delta\mathrm{Red}_\tau^V$ [e cm]		$\delta\mathrm{Imd}_\tau^V$ [e cm]	
	$E_{ab}[T_{33}]$	$E_{ab}[\mathcal{O}_{\mathrm{Red}_\tau}]$	$E_{ab}[\hat{O}_{33}]$	$E_{ab}[\mathcal{O}_{\mathrm{Im}\,d_\tau}]$
$\sqrt{s} = 3.686$ GeV ($N_{\tau^+\tau^-} = 3.5 \times 10^6$)	4.11×10^{-16}	4.87×10^{-17}	2.97×10^{-16}	2.40×10^{-17}
$\sqrt{s} = 5.6$ GeV ($N_{\tau^+\tau^-} = 5.5 \times 10^7$)	1.78×10^{-17}	2.93×10^{-18}	6.52×10^{-18}	1.42×10^{-18}
$\sqrt{s} = 10.58$ GeV ($N_{\tau^+\tau^-} = 5.5 \times 10^{10}$)	2.93×10^{-19}	9.42×10^{-20}	5.08×10^{-20}	2.43×10^{-20}
$\sqrt{s} = m_Z$ ($N_{\tau^+\tau^-} = 1.2 \times 10^{11}$)	3.67×10^{-21}	1.12×10^{-21}	4.36×10^{-20}	1.78×10^{-21}

TABLE III. Same as Table II, but including γ-Z interference effect.

	$\delta\mathrm{Red}_\tau^Z$ [e cm]		$\delta\mathrm{Imd}_\tau^Z$ [e cm]	
	E_{ab} [SO_1[a]]	$E_{ab}[OO_1]$	$E_{ab}[SO_2]$	$E_{ab}[OO_2]$
$\sqrt{s}=m_Z$ ($N_{\tau^+\tau^-}=1.2\times10^{11}$)	4.94×10^{-20}	1.13×10^{-21}	9.32×10^{-21}	1.79×10^{-21}

[a]SO_i and OO_i (i = 1, 2) are simple and optimal observables denoted in Eqs. (34) and (36).

for the imaginary component, respectively. Reference [44] gives sensitivities for both real and imaginary components of the τ lepton's EDM at BEPCII $\sqrt{s}=4.18$ GeV and 4.95 GeV. Given planned collider upgrades and proposed running energies scenarios, renewed numerical theoretical predictions are required. When the energy increases to $\sqrt{s}=10.58$ GeV, the $\delta\mathrm{Red}_\tau^\gamma$ and $\delta\,\mathrm{Im}\,d_\tau^\gamma$ improve by approximately three orders of magnitude, reaching 10^{-20} e cm. Our results are consistent with ref. [36], with the slight discrepancy attributed to differences in the input parameters. For the WDM of τ lepton, the numbers show that the sensitivity to d_τ^Z at CEPC can reach the level of 10^{-21} e cm using $\mathcal{O}_{\mathrm{Re}d_\tau}$ and $\mathcal{O}_{\mathrm{Im}\,d_\tau}$. This is sufficient to be sensitive to certain BSM that predict values for d_τ^Z of the order 10^{-19} e cm (See, e.g., [45,46]). Compared to the simple observables, the sensitivity to $\mathrm{Re}[d_\tau^Z]$ is improved by more than a factor three with $\mathcal{O}_{\mathrm{Re}d_\tau}$ while the sensitivity to $\mathrm{Im}[d_\tau^Z]$ is improved by more than a factor twenty.

Due to the small value of the WDM, we further assess how photon-Z boson interference in process (4) influences the WDM sensitivity. The coefficients $c, c', r, r', w, w', t, t'$ and the expectation values occurring in Eqs. (33)–(36) for simple observables and optimal observables are calculated numerically. These results are shown in Appendix Tables VIII–X. The resulting 1 s.d. sensitivity, based on the number of events given in scenario IV, are given in Table III. Comparing scenario IV results between Tables II and III, both components of τlepton$'$ WDM exhibit marginal sensitivity degradation when using optimal observables, while simple observables show different behavior: the real component sensitivity degrades substantially, whereas the imaginary component sensitivity improves.

B. AMDM results

Considering the high statistics of the τ pairs, we study the AMDM of τ lepton at $\sqrt{s}=10.58$ GeV in the Belle-II experiment. We assume that $N_{\tau\tau}=4.5\times10^{10}$ τ-pair events can be eventually recorded. After diagonalizing the coefficient matrix, we calculate the expectation values of the simple observables T_a^{ij}, $\hat{O}_a^{ij}$ and optimal observables $\mathcal{O}_{\mathrm{Re}a_\tau}$, $\mathcal{O}_{\mathrm{Im}\,a_\tau}$. In Tables IV and V, we give results of the 1 s.d. sensitivities to the real and imaginary components of the τ AMDM calculated using the differential cross section at SM tree level. The optimal observables in this table are defined by tree level S_0. Comparing the data from those two tables, the sensitivity of optimal observables is of the order of 10^{-5}, an order of magnitude higher than that of the simple observable. Thanks to a large branching ratio and spinor analyzing power, the precision resulting from $\tau^-\to\nu\pi^0\pi^-$, $\tau^+\to\nu\pi^0\pi^+$ and $\tau^-\to\nu\pi^0\pi^-$, $\tau^+\to\bar{\nu}\nu\ell^+$ final state is very high and can reach 4.23×10^{-5} and 3.71×10^{-5}, respectively. Combining these 1 s.d. listed in Tables IV and V in quadratures, one gets the 1 s.d. sensitivity $\delta\mathrm{Rea}_\tau^\gamma$ and $\delta\mathrm{Ima}_\tau^\gamma$ shown in Table VI. The sensitivity of optimal observables yields a factor of three improvement in precision compared to simple one for the real component of $a_\tau^{\gamma,NP}$, while for the imaginary component of $a_\tau^{\gamma,NP}$, there is an improvement by a factor of about seven. The sensitivity of $\mathcal{O}_{\mathrm{Im}\,a_\tau}$ reaches 1.76×10^{-5} and of $\mathcal{O}_{\mathrm{Re}a_\tau}$ reaches 1.88×10^{-5}.

As is well known, the expectation values of $\mathcal{O}_{\mathrm{Re}a_\tau}$ and $\mathcal{O}_{\mathrm{Im}\,a_\tau}$ receive contributions from both SM interactions and potential NP. If the effect of $a_\tau^{\gamma,SM}$ on the expectation value

TABLE IV. Simple observables T_a^{33}, $\hat{O}_a^{33}$ for the $e^+e^-\to\gamma^*\to\tau\tau$ at Belle-II with $\sqrt{s}=10.58$ GeV. For the decay modes where leptons are involved the cross section is the sum of the respective cross sections for $\ell=e$ and μ.

$\tau^-\to$	$\tau^+\to$	κ_γ (GeV^3)	$\sqrt{V'_{ab}(T_a^{33})}$ (GeV^3)	$\delta\mathrm{Ima}_\tau^\gamma$ (10^{-4})	$\bar{\kappa}_\gamma$	$\sqrt{V'_{ab}(\hat{O}_a^{33})}$	$\delta\mathrm{Rea}_\tau^\gamma$ (10^{-4})
$\nu\pi^-$	$\bar{\nu}\pi^+$	1.21	3.34	3.61	−0.200	0.640	4.19
$\nu\rho^-$	$\bar{\nu}\rho^+$	0.295	2.61	4.91	−0.301	0.612	1.13
$\nu\bar{\nu}\ell^-$	$\bar{\nu}\nu\ell^+$	−0.099	1.69	6.96	−0.222	0.651	1.19
$\nu\bar{\nu}\ell^-$	$\bar{\nu}\pi^+$	−0.236	2.77	6.05	−0.238	0.646	1.40
$\nu\bar{\nu}\ell^-$	$\bar{\nu}\rho^+$	−0.403	2.57	2.14	−0.264	0.637	0.811
$\nu\pi^-$	$\bar{\nu}\rho^+$	−0.903	3.18	2.12	0.257	0.630	1.48

TABLE V. Same as Table IV, but for optimal observables $\mathcal{O}_{\mathrm{Re}a_\tau}$ and $\mathcal{O}_{\mathrm{Im}\,a_\tau}$.

$\tau^-\to$	$\tau^+\to$	ξ_γ	$\sqrt{V'_{ab}(\mathcal{O}_{\mathrm{Re}a_\tau})}$	$\delta\mathrm{Rea}_\tau^\gamma$ (10^{-5})	ξ'_γ	$\sqrt{V'_{ab}(\mathcal{O}_{\mathrm{Im}\,a_\tau})}$	$\delta\mathrm{Ima}_\tau^\gamma$ (10^{-5})
$\nu\pi^-$	$\bar{\nu}\pi^+$	0.191	0.437	9.97	0.186	0.432	10.1
$\nu\pi^0\pi^-$	$\nu\pi^0\pi^+$	0.191	0.437	4.22	0.186	0.432	4.23
$\nu\pi^-\pi^-\pi^+$	$\nu\pi^+\pi^+\pi^-$	0.191	0.437	11.5	0.186	0.432	11.7
$\nu\pi^0\pi^-$	$\bar{\nu}\pi^+$	0.191	0.437	4.59	0.186	0.432	4.65
$\nu\pi^-\pi^-\pi^+$	$\bar{\nu}\pi^+$	0.191	0.437	7.60	0.186	0.432	7.70
$\nu\pi^-\pi^-\pi^+$	$\nu\pi^0\pi^+$	0.191	0.437	4.94	0.186	0.432	5.01
$\nu\bar{\nu}\ell^-$	$\bar{\nu}\nu\ell^+$	0.036	0.190	7.12	0.031	0.177	7.65
$\nu\pi^-$	$\bar{\nu}\nu\ell^+$	0.060	0.244	7.04	0.091	0.301	5.70
$\nu\pi^0\pi^-$	$\bar{\nu}\nu\ell^+$	0.060	0.244	4.58	0.091	0.301	3.71
$\nu\pi^-\pi^-\pi^+$	$\bar{\nu}\nu\ell^+$	0.060	0.244	7.58	0.091	0.301	6.14

TABLE VI. 1 s.d. sensitivity on $\mathrm{Re}[a_\tau^\gamma]$ and $\mathrm{Im}[a_\tau^\gamma]$ obtained from the combined decay channels.

$\delta\mathrm{Rea}_\tau^\gamma$		$\delta\mathrm{Ima}_\tau^\gamma$	
$E_{ab}[\hat{O}_a^{33}]$	$E_{ab}[\mathcal{O}_{\mathrm{Re}a_\tau}]$	$E_{ab}[T_a^{33}]$	$E_{ab}[\mathcal{O}_{\mathrm{Im}\,a_\tau}]$
4.98×10^{-5}	1.88×10^{-5}	1.28×10^{-4}	1.76×10^{-5}

TABLE VII. The sensitivity to $a_\tau^{\gamma,SM}$ by measuring $\mathcal{O}_{\mathrm{Re}a_\tau}$.

$a_\tau^{\gamma,SM}$ $(\times10^{-3})$	$E_0[\mathcal{O}_{\mathrm{Re}a_\tau}]$	$\xi^{\mathrm{Re}a_\tau}$	$\delta\mathrm{Rea}_\tau$
0	0.9539	0.1915	4.225×10^{-5}
1.17721	0.9542	0.1911	4.237×10^{-5}
1.17717	0.9542	0.1911	4.237×10^{-5}
1.17713	0.9542	0.1911	4.237×10^{-5}

exceeds the statistical uncertainty of the measurement, then the SM contribution can be constrained by measuring $E^{ab}[\mathcal{O}]$. $E^{ab}[\mathcal{O}]$ can be fitted with a linear function of $a_\tau^{V,NP}$

$$E^{ab}[\mathcal{O}_i]=\xi^i a_{\tau,i}^{\gamma,NP}+b^i,\quad (i=\mathrm{Re}a_\tau,\mathrm{Im}\,a_\tau),\quad (38)$$

where ξ^i is the slope and b^i corresponds to the SM expectation value of $\mathcal{O}_i$. For the decay channel $\tau^-\to\nu\pi^0\pi^-,\tau^+\to\nu\pi^0\pi^+$, tree level differential cross section gives $E_0[\mathcal{O}_{\mathrm{Re}a_\tau}]=0.9539$ with a slope of 0.1915. In the SM, the differential cross section related to $a_\tau^{\gamma,SM}$ can be factorized into $a_\tau^{\gamma,SM}S_{1,\mathrm{Re}a_\tau}$ which has the same effective vertex as $a_\tau^{\gamma,NP}$. Using the SM prediction value of a_τ $a_\tau^{\gamma,SM}=(1.177171\pm0.000039)\times10^{-3}$, we derive the bounds on $\xi^{\mathrm{Re}a}$, $b^{\mathrm{Re}a}$ and sensitivity by varying $a_\tau^{\gamma,SM}$ within its uncertainty range, shown in Table VII. Our results indicate that the observables defined as $S_{1,\mathrm{Re}a_\tau}/S_0$ can not identify $a_\tau^{\gamma,NP}$ from $a_\tau^{\gamma,SM}$ within the current sensitivity limits.

V. SUMMARY

The precise measurement of the τ lepton's electric(weak) dipole moment and anomalous magnetic dipole moment provide a powerful probe for testing the SM and uncovering NP. Electron-positron colliders offer an ideal place for these studies. With ongoing advancements in both the collider energy and luminosity, e^+e^- facilities will produce large datasets of $\tau^+\tau^-$, hence the search for τ E(W)DM and AMDM will enter a precision era.

In this work, we study τ pair production in e^+e^- collisions with subsequent decays of $\tau^\pm$ to (semi)leptonic or hadronic channels in various scenarios. For all one-prong and multi-prongs decay channels considered, we take the full kinematic information of the final-states system into account by incorporating the respective differential τ lepton decay density matrix into its production density matrix. The one standard deviation sensitivity to the real and imaginary components of E(W)DM and AMDM are estimated through both simple and optimal observables, with comprehensive analysis of their expectation values and covariance.

At BEPC II, optimal observables yield an order of magnitude improvement in precision over simple observables for measurements of real and imaginary components of the τ EDM at center-of-mass energies of 3.686 GeV and 5.6 GeV. Specifically, with 3.5×10^6 τ pair production at $\sqrt{s}=3.686$ GeV, the sensitivities derived from optimal observables read $\delta\mathrm{Red}_\tau^\gamma=4.87\times10^{-17}$ e cm and $\delta\mathrm{Imd}_\tau^\gamma=2.40\times10^{-17}$ e cm, with further enhancement at higher energies. For Belle-II, our results project the precisions of 9.42×10^{-20} e cm and 2.43×10^{-20} e cm for $\mathrm{Re}[d_\tau^\gamma]$ and $\mathrm{Im}[d_\tau^\gamma]$, respectively, while for AMDM $\delta\mathrm{Rea}_\tau^\gamma=1.88\times10^{-5}$ and $\delta\mathrm{Ima}_\tau^\gamma=1.76\times10^{-5}$. CEPC has the capability to measure τ lepton WDM with precisions reaching the level of 10^{-21} e cm, with specific values of $\delta\mathrm{Red}_\tau^Z=1.12\times10^{-21}$ and $\delta\mathrm{Imd}_\tau^Z=1.78\times10^{-21}$ at the Z mass energy, which is sufficient to be sensitive to certain BSM models. Precision measurement of the τ lepton's electromagnetic moments using optimal observables at current and future electron-positron colliders will provide significant information about physics beyond the Standard Model, offering high sensitivity to leptonic CP violation.

ACKNOWLEDGMENTS

The authors sincerely thank Professor Werner Bernreuther, Long Chen for their invaluable discussions and comments of this manuscript, and the members of the Institute of theoretical physics of Shandong University for helpful communications. This work is supported in part by National Natural Science Foundation of China under the Grants No. 12235008, No. 12321005 and No. 12405121.

DATA AVAILABILITY

The data are not publicly available. The data are available from the authors upon reasonable request.

APPENDIX

In this Appendix, we present numerical results for the coefficients, the expectation values, and the 1 s.d. ideal statistical error of both simple and optimal observables across different τ lepton decay channels in scenario IV. These quantities are defined in Eqs. (33)–(36). Within our numerical uncertainties, the coefficients r_γ, r'_γ for simple observables and t_γ, t'_γ for optimal observables vanish. This is consistent with the dominance of Z boson exchange at the Z-pole energy.

TABLE VIII. Simple observables T^{ij}, $\hat{A}_1$ at $\sqrt{s} = m_Z$ including γ-Z interference effects.

$\tau^- \to$	$\tau^+ \to$	c_γ (GeV^3)	c_Z (GeV^3)	$\sqrt{E_0^{ab}[T_{33}^2]}$ (GeV^3)	r_Z (10^{-3})	$\sqrt{E_0^{ab}[\hat{A}_1^2]}$	$E_0^{ab}[T_{33}\hat{A}_1]$ (GeV^3)	$\delta\mathrm{Red}_\tau^Z$ (10^{-19} e cm)
$\nu\pi^-$	$\bar{\nu}\pi^+$	2.06	−1349	771	−22.3	0.517	16.4	1.35
$\nu\rho^-$	$\bar{\nu}\rho^+$	0.327	−661	781	3.14	0.540	−1.38	4.22
$\nu\bar{\nu}\ell^-$	$\bar{\nu}\nu\ell^+$	0.166	247	382	−10.2	0.545	−9.20	0.958
$\nu\bar{\nu}\ell^-$	$\bar{\nu}\pi^+$	−0.585	−240	548	18.9	0.558	−1.42	0.672
$\nu\bar{\nu}\ell^-$	$\bar{\nu}\rho^+$	−0.235	66.7	561	3.42	0.552	−6.43	2.39
$\nu\pi^-$	$\bar{\nu}\rho^+$	0.824	−1103	790	1.09	0.534	6.06	13.0

TABLE IX. Same as Table VIII, but for simple observables $\hat{O}^{ij}$, $\hat{A}_2$.

$\tau^- \to$	$\tau^+ \to$	c'_γ (10^{-4})	c'_Z (10^{-3})	$\sqrt{E_0^{ab}[\hat{O}_{33}^2]}$ (10^{-2})	r'_Z (10^{-3})	$\sqrt{E_0^{ab}[\hat{A}_2^2]}$ (10^{-2})	$E_0^{ab}[\hat{O}_{33}\hat{A}_2]$ (10^{-4})	$\delta\mathrm{Imd}_\tau^Z$ (10^{-20} e cm)
$\nu\pi^-$	$\bar{\nu}\pi^+$	−4.97	−15.5	11.4	−12.8	5.97	7.36	2.69
$\nu\rho^-$	$\bar{\nu}\rho^+$	−1.20	−3.75	4.01	3.09	2.07	−0.399	1.64
$\nu\bar{\nu}\ell^-$	$\bar{\nu}\nu\ell^+$	1.74	5.44	13.9	−4.49	7.87	0.957	3.15
$\nu\bar{\nu}\ell^-$	$\bar{\nu}\pi^+$	−1.62	−5.06	12.5	4.16	6.81	−3.18	3.73
$\nu\bar{\nu}\ell^-$	$\bar{\nu}\rho^+$	0.271	0.848	10.2	−0.700	5.72	0.293	12.1
$\nu\pi^-$	$\bar{\nu}\rho^+$	−3.08	−9.65	8.47	7.95	4.39	−3.89	1.47

TABLE X. Same as Table VIII, but for optimal observables $\mathcal{O}^Z_{\mathrm{Re}d_\tau}$ and $\mathcal{O}^Z_{\mathrm{Im}\,d_\tau}$.

$\tau^- \to$	$\tau^+ \to$	t_Z	$\sqrt{E_0^{ab}[\mathcal{O}^Z_{\mathrm{Re}d_\tau}]}$	t'_Z	$\sqrt{E_0^{ab}[\mathcal{O}^Z_{\mathrm{Im}\,d_\tau}]}$	$\delta\mathrm{Red}_\tau^Z$ (10^{-21} e cm)	$\delta\mathrm{Imd}_\tau^Z$ (10^{-21} e cm)
$\nu\pi^-$	$\bar{\nu}\pi^+$	0.830	0.911	0.368	0.606	6.35	9.54
$\nu\pi^0\pi^-$	$\nu\pi^0\pi^+$	0.830	0.911	0.368	0.606	2.69	4.04
$\nu\pi^-\pi^-\pi^+$	$\nu\pi^+\pi^+\pi^-$	0.830	0.911	0.368	0.606	7.37	11.1
$\nu\pi^0\pi^-$	$\bar{\nu}\pi^+$	0.830	0.911	0.368	0.606	2.92	4.39
$\nu\pi^-\pi^-\pi^+$	$\bar{\nu}\pi^+$	0.830	0.911	0.368	0.606	4.84	7.26
$\nu\pi^-\pi^-\pi^+$	$\nu\pi^0\pi^+$	0.830	0.911	0.368	0.606	3.15	4.73
$\nu\bar{\nu}\ell^-$	$\bar{\nu}\nu\ell^+$	0.123	0.350	0.0387	0.197	5.12	9.12
$\nu\pi^-$	$\bar{\nu}\nu\ell^+$	0.365	0.604	0.126	0.354	3.77	6.43
$\nu\pi^0\pi^-$	$\bar{\nu}\nu\ell^+$	0.365	0.604	0.126	0.354	2.45	4.18
$\nu\pi^-\pi^-\pi^+$	$\bar{\nu}\nu\ell^+$	0.365	0.604	0.126	0.354	4.06	6.92

[1] M. Kobayashi and T. Maskawa, Prog. Theor. Phys. **49**, 652 (1973).
[2] Y. Yamaguchi and N. Yamanaka, Phys. Rev. Lett. **125**, 241802 (2020).
[3] Y. Yamaguchi and N. Yamanaka, Phys. Rev. D **103**, 013001 (2021).
[4] T. S. Roussy, L. Caldwell, T. Wright, W. B. Cairncross, Y. Shagam, K. B. Ng, N. Schlossberger, S. Y. Park, A. Wang, J. Ye *et al.*, Science **381**, adg4084 (2023).
[5] G. W. Bennett *et al.* (Muon (g-2) Collaboration), Phys. Rev. D **80**, 052008 (2009).
[6] W. Bernreuther, A. Brandenburg, and P. Overmann, Phys. Lett. B **391**, 413 (1997); **412**, 425(E) (1997).
[7] S. Navas *et al.* (Particle Data Group), Phys. Rev. D **110**, 030001 (2024).
[8] K. Inami *et al.* (Belle Collaboration), J. High Energy Phys. 04 (2022) 110.
[9] W. Lohmann, Nucl. Phys. B, Proc. Suppl. **144**, 122 (2005).
[10] T. Kinoshita, Int. J. Mod. Phys. A **29**, 1430003 (2014).
[11] R. H. Parker, C. Yu, W. Zhong, B. Estey, and H. Müller, Science **360**, 191 (2018).
[12] G. W. Bennett *et al.* (Muon g-2 Collaboration), Phys. Rev. D **73**, 072003 (2006).
[13] B. Abi *et al.* (Muon g-2 Collaboration), Phys. Rev. Lett. **126**, 141801 (2021).
[14] D. P. Aguillard *et al.* (Muon g-2 Collaboration), Phys. Rev. Lett. **131**, 161802 (2023).
[15] T. Aoyama, N. Asmussen, M. Benayoun, J. Bijnens, T. Blum, M. Bruno, I. Caprini, C. M. Carloni Calame, M. Cè, G. Colangelo *et al.*, Phys. Rep. **887**, 1 (2020).
[16] L. Cotrozzi (Muon g-2 Collaboration), Nuovo Cimento Soc. Ital. Fis. **47C**, 282 (2024).
[17] B. C. Toth, S. Borsanyi, Z. Fodor, J. Guenther, C. Hoelbling, S. D. Katz, L. Lellouch, T. Lippert, K. Miura, L. Parato *et al.*, Proc. Sci., LATTICE2021 (**2022**) 005.
[18] P. Masjuan, A. Miranda, and P. Roig, Proc. Sci., QNP2024 (**2025**) 216 [arXiv:2411.09811].
[19] R. Aliberti, T. Aoyama, E. Balzani, A. Bashir, G. Benton, J. Bijnens, V. Biloshytskyi, T. Blum, D. Boito, M. Bruno *et al.*, Phys. Rep. **1143**, 1 (2025).
[20] S. P. Martin and J. D. Wells, Phys. Rev. D **64**, 035003 (2001).
[21] A. Hayrapetyan *et al.* (CMS Collaboration), Rep. Prog. Phys. **87**, 107801 (2024).
[22] A. Keshavarzi, D. Nomura, and T. Teubner, Phys. Rev. D **101**, 014029 (2020).
[23] T. Abe *et al.* (Belle-II Collaboration), arXiv:1011.0352.
[24] E. Kou *et al.* (Belle-II Collaboration), Prog. Theor. Exp. Phys. **2019**, 123C01 (2019); **2020**, 029201(E) (2020).
[25] M. Ablikim *et al.* (BESIII Collaboration), Chin. Phys. C **48**, 093001 (2024).
[26] H. B. Li *et al.* (BESIII Collaboration), arXiv:2204.08943.
[27] J. B. Guimarães da Costa *et al.* (CEPC Study Group), arXiv:1811.10545.
[28] H. Cheng *et al.* (CEPC Physics Study Group), arXiv:2205.08553.
[29] D. Atwood and A. Soni, Phys. Rev. D **45**, 2405 (1992).
[30] M. Diehl and O. Nachtmann, Z. Phys. C **62**, 397 (1994).
[31] G. Aad *et al.* (ATLAS Collaboration), Phys. Lett. B **805**, 135426 (2020).
[32] G. Aad *et al.* (ATLAS Collaboration), J. High Energy Phys. 05 (2024) 105.
[33] A. M. Sirunyan *et al.* (CMS Collaboration), Phys. Rev. D **104**, 052004 (2021).
[34] S. Jahedi, J. Lahiri, and A. Subba, J. High Energy Phys. 07 (2025) 280.
[35] G. Abbiendi *et al.* (OPAL Collaboration), Eur. Phys. J. C **33**, 463 (2004).
[36] W. Bernreuther, L. Chen, and O. Nachtmann, Phys. Rev. D **103**, 096011 (2021).
[37] X. Chen and Y. Wu, J. High Energy Phys. 10 (2019) 089.
[38] X. G. He, C. W. Liu, J. P. Ma, C. Yang, and Z. Y. Zou, J. High Energy Phys. 04 (2025) 001.
[39] K. Bhide and V. Lang, arXiv:2410.23070.
[40] S. Banerjee, A. Y. Korchin, E. Richter-Was, and Z. Was, Phys. Rev. D **109**, 013002 (2024).
[41] D. Shao, B. Yan, S. R. Yuan, and C. Zhang, Sci. China Phys. Mech. Astron. **67**, 281062 (2024).
[42] D. Y. Shao, H. Xiang, F. Xu, B. Yan, and C. Zhang, arXiv:2506.15245.
[43] W. Bernreuther, O. Nachtmann, and P. Overmann, Phys. Rev. D **48**, 78 (1993).
[44] W. Bernreuther, L. Chen, and O. Nachtmann, Phys. Rev. D **104**, 115002 (2021).
[45] P. Poulose and S. D. Rindani, Pramana **51**, 387 (1998).
[46] T. Huang, W. Lu, and Z. j. Tao, Phys. Rev. D **55**, 1643 (1997).